Characterization of a *Rhodobacter capsulatus* Reaction Center Mutant that Enhances the Distinction between Spectral Forms of the Initial Electron Donor†

J. Elizabeth Eastman, Aileen K. W. Taguchi, Su Lin, Jonathon A. Jackson, and Neal W. Woodbury*

Department of Chemistry and Biochemistry and the Center for the Study of Early Events in Photosynthesis, Arizona State University, Tempe, Arizona 85287-1604

Received March 7, 2000; Revised Manuscript Received July 24, 2000

ABSTRACT: A large scale mutation of the *Rhodobacter capsulatus* reaction center M-subunit gene, *sym2-1*, has been constructed in which amino acid residues M205−M210 have been changed to the corresponding L subunit amino acids. Two interconvertable spectral forms of the initial electron donor are observed in isolated reaction centers from this mutant. Which conformation dominates depends on ionic strength, the nature of the detergent used, and the temperature. Reaction centers from this mutant have a ground-state absorbance spectrum that is very similar to wild-type when measured immediately after purification in the presence of high salt. However, upon subsequent dialysis against a low ionic strength buffer or the addition of positively charged detergents, the near-infrared spectral band of P (the initial electron donor) in *sym2-1* reaction centers is shifted by over 30 nm to the blue, from 852 to 820 nm. Systematically varying either the ionic strength or the amount of charged detergent reveals an isobestic point in the absorbance spectrum at 845 nm. The wild-type spectrum also shifts with ionic strength or detergent with an isobestic point at 860 nm. The large spectral separation between the two dominant conformational forms of the *sym2-1* reaction center makes detailed measurements of each state possible. Both of the spectral forms of P bleach in the presence of light. Electrochemical measurements of the P/P+ midpoint potential of *sym2-1* reaction centers show an increase of about 30 mV upon conversion from the long-wavelength form to the short-wavelength form of the mutant. The rate constant of initial electron transfer in both forms of the mutant reaction centers is essentially the same, suggesting that the spectral characteristics of P are not critical for charge separation. The short-wavelength form of P in this mutant also converts to the long-wavelength form as a function of temperature between room temperature and 130 K, again giving rise to an isobestic point, in this case at 838 nm for the mutant. A similar, though considerably less pronounced spectral change with temperature occurs in wild-type reaction centers, with an isobestic point at about 855 nm, close to that found by titrating with ionic strength or detergent. Fitting the temperature dependence of the *sym2-1* reaction center spectrum to a thermodynamic model resulted in a value for the enthalpy of the conformational interconversion between the short- and long-wavelength forms of about −6 kJ/mol and an entropy of interconversion of about −35 J/(K mol). Similar values of enthapy and entropy changes can be used to model the temperature dependence in wild-type. Thus, much of the temperature dependence of the reaction center special pair near-infrared absorbance band can be described as an equilibrium shift between two spectrally distinct conformations of the reaction center.

The photosynthetic reaction centers of purple nonsulfur bacteria have three protein subunits (L, M, and H) and 10 noncovalently bound cofactors. There are four bacteriochlorophylls, two bacteriopheophytins, two quinones, one iron atom, and a carotenoid (*1*−*4*). The primary solar energy conversion event in the reaction center is transmembrane charge separation. Upon excitation, the primary electron donor (P),[1] which is a dimer of bacteriochlorophylls, transfers an electron through a neighboring monomer bacteriochlorophyll (B_A) to a bacteriopheophytin (H_A) in a few picoseconds and then on to a quinone (Q_A) in about 200 ps (*5*−*12*).

The X-ray structures of the reaction centers from *Rhodobacter sphaeroides* and *Rhodopseudomonas viridis* have been determined (*1*−*3*, *13*). No structure has been obtained for the reaction center from *Rhodobacter capsulatus*, but it is presumed to be very similar to the *Rb. sphaeroides* structure based on the high amino acid homology between the L and M subunits of the two species (*14*−*16*). The most prominent structural components of the reaction center protein are five hydrophobic helices in each of the L and M subunits that span the membrane in vivo. The backbone structure of the L and M subunits and the positions of the associated cofactors have a high degree of 2-fold rotational symmetry.

† This work was supported by Grants MCB-9513457-004 and MCB-9817388 from the National Science Foundation.

* To whom correspondence should be addressed.

[1] Abbreviations: *Rb*., *Rhodobacter*; *Rp*. *Rhodopseudomonas*; *Rs*. *Rhodospirillum*; P, primary electron donor; B, monomer bacteriochlorophyll; H bacteriopheophytin; Q, quinone; LDAO, *N*,lauryl-*N*,*N*-dimethylamine-*N*-oxide; buffer B, 10 mM potassium phosphate, pH 7.8, with 0.05% LDAO; BTP, Bis-Tris propane; AMP, 2-amino-2-methyl-1-propanol; DOC, deoxycholate; CTAB, cetyltrimethylammonium bromide; E_M, midpoint redox potential.

10.1021/bi0005254 CCC: $19.00
Published on Web 11/08/2000

Interestingly, only one of the two potential electron-transfer pathways defined by this quasi-symmetric structure appears to play a major electron-transfer role in vivo (*6*, *11*, *17*−*20*).

In membrane-bound reaction centers of *Rb. capsulatus*, the long-wavelength transition of P is centered at about 860 nm when expressed in a U43 background (*21*). Similarly in *Rb. sphaeroides*, the P transition in membrane-bound reaction centers is at 860 nm (*22*). The optical and photochemical properties of isolated reaction centers depend on experimental conditions (*23*). The peak position of the long-wavelength, near-infrared absorption band (the Q_Y band) of P varies by up to 15 nm depending on ubiquinone content, the detergent used in the preparation, and the type of protocol used (*24*, *25*). It has also been observed that in reaction centers solubilized in *N*-lauryl-*N*,*N*-dimethylamine-*N*-oxide (LDAO), the Q_Y band of P in Bchl*a*-containing reaction centers from different species is located at either 865 or 855 nm, leading to the suggestion that reaction centers fall into two classes. One class (P band at 865 nm) includes LDAO isolated reaction centers from *Rb. sphaeroides* and *Rb. rubrum*. The second class (P band at 855 nm.) includes LDAO isolated reaction centers from *Rb. capsulatus* and *Rs. centenum* (*26*). Wang et al. also found that it is possible to convert the reaction centers from one spectral form, or class, to another by the addition of certain ionic detergents (*26*). Removal of all detergent causes the Q_Y band of P to shift from 865 to 846 nm in reaction centers from *Rb. sphaeroides* (*27*). Air-dried films of aqueous suspensions of *Rb. sphaeroides* reaction centers on glass or quartz plates have shown a blueshift in the P band from 860 to 845 nm (*24*). The Q_Y P band position has also been found to depend on the ubiquinone-50 content of the Q_B site of reaction centers and LM particles (lacking the H subunit) from *Rb. sphaeroides* (*25*).

ENDOR/TRIPLE spectroscopy of reaction centers from *Rb. sphaeroides* has revealed two distinct forms of P^+, one is due to a population of reaction centers in which ground-state P has a maximum long-wavelength absorbance at 850 nm and one is due to a different population with a P transition at 866 nm (*28*). The two forms of P^+ in *Rb. capsulatus* have been found to have different spin density ratios (fraction of electron density on P_L versus P_M) as well as different $P^+Q_A^-$ recombination rates (*29*). A persistent structural transformation of P can be produced by light alone in *Rp. viridis* reaction centers (*30*). Kalman and Maroti have also observed a light-induced conformational change in reaction centers between two forms that have different amounts of proton release (*31*). A comparison of trypsin treatment of *Rb. sphaeroides* and *Rp. viridis* reaction centers in the dark and under illumination also reveal light-induced structural changes (*32*, *33*).

The spectral properties of the photosynthetic reaction centers from purple nonsulfur bacteria are quite temperature sensitive. In particular, the Q_Y transition of P shifts significantly to the red as the temperature is lowered. In reaction centers isolated from the bacterium *Rb. capsulatus*, the peak of the Q_Y transition of P is about 850 nm at room temperature and shifts to about 875 nm at 10 K. Triplet-minus-singlet absorbance difference spectra of reaction centers from a related bacterium, *Rb. sphaeroides*, have shown a shift in the Q_Y band of P from 861 nm at 290 K to 890 nm upon cooling to 24 K (*34*). Overlaid triplet-minus-singlet spectra at various temperatures revealed an isobestic point at 873 nm (*34*). The authors concluded that this indicated not a shift, but a stabilization at low temperature of a conformation of the special pair that absorbs at longer wavelength (*34*).

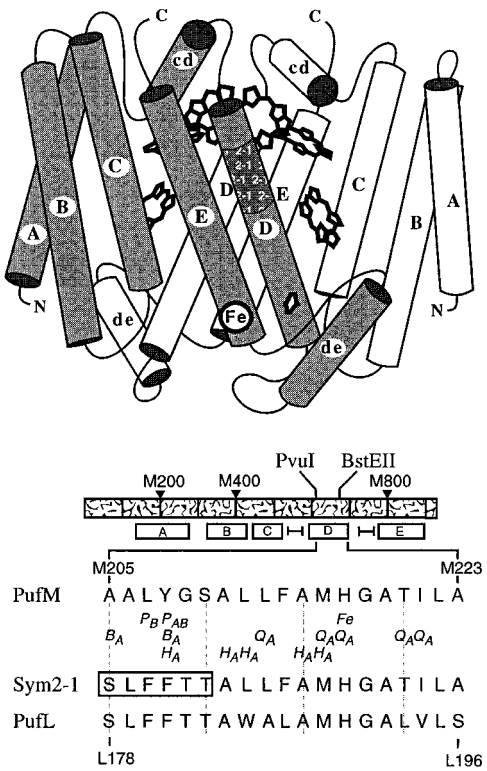

FIGURE 1: Top portion of the figure is a diagrammatic representation of the structure of the photosynthetic reaction center showing the approximate relationship between the cofactors and the L (light) and M (dark) subunits. The tubes represent α-helices. The region labeled "2-1" on helix D of the M subunit corresponds to the region mutated in *sym2-1*. This scheme is based on the X-ray crystal structures of *Rb. sphaeroides* and *Rp. viridis*, and a very similar representation of the *Rp. viridis* structure from Michel and Deisenhofer (*65*). The bottom shows the region of the M gene altered in *sym2-1* and the specific amino acid changes involved. The DNA sequence of the *pufM* gene is represented by the mezzotinted rectangle with the nucleotide positions indicated at 200 base intervals. The locations of the α-helices in the *pufM* gene product as determined from the *Rb. sphaeroides* X-ray structure are shown below the gene. The amino acid sequences for the PufM, Sym2-1, and PufL proteins are shown in the lower part of the figure applying the alignment of Michel et al. (*66*). Cofactors which appear within 4 Å of a particular M subunit residue are shown below the *Rb. capsulatus* M subunit sequence. Distance information was compiled from crystallographic data (*67*, *68*).

In this report, we describe the spectral characterization of *sym2-1*, a *Rb. capsulatus* symmetry mutation, as a function of the detergent identity, ionic strength, and temperature. The *sym2-1* mutation was generated as one in a series of mutants which increase the protein symmetry surrounding the redox-active cofactors (*35*−*38*). This mutation greatly enhances the difference between the two spectral forms of P previously observed in wild-type (*26*), allowing a more detailed characterization of the differences between the two forms.

EXPERIMENTAL PROCEDURES

Strains and Plasmid Constructions. The mutation, *sym2-1*, is shown in Figure 1. Six consecutive amino acids in the M-subunit of the reaction center have been replaced by their counterparts in the L-subunit. Figure 1 also diagrams the

corresponding region of the reaction center structure based on the X-ray crystal structures of *Rp. viridis* and *Rb. sphaeroides* reaction centers (*1*−*3*, *13*). The *sym2-1* mutant was constructed as previously described (*37*).

Chromatophore and Reaction Center Isolation. Reaction centers were isolated from a U43 transconjugant containing either the plasmid pCR (a derivative of pU2922) which contains the wild-type *puf* operon (*35*, *39*, *40*) or pLEP3, a pCR-based construct containing the *sym2-1* mutation (*37*). U43(pCR) was employed as the pseudo-wild-type for this study.

Wild-type and mutant cells were grown in RCVPY/kan medium (*41*), harvested by low-speed centrifugation, resuspended in 10 mM potassium phosphate buffer, pH 7.8, and disrupted by two passes through a French pressure cell at 20 000 psi. Chromatophores were then isolated by differential centrifugation essentially as described by Prince and Youvan (*42*) and modified by Xiao (*41*). Reaction centers were isolated as in ref *37*, with the following modifications. The pH of the isolation buffer was raised to 7.8 in order to maximize yields. A continuous salt gradient from 0 to 350 mM KCl in buffer B (10 mM potassium phosphate, pH 7.8, with 0.05% LDAO) was applied to crude reaction centers bound to the DEAE sephacel column, rather than incrementally stepping up the ionic strength as described previously. In addition, the higher detergent wash step (0.6% LDAO) after the reaction centers were bound to the column was omitted. This step was omitted because it significantly decreased reaction center yields for the mutant. Peak fractions were pooled, concentrated, and then dialyzed against buffer B at a volume ratio of 1:200. Aliquots were stored at −80° C for later use. Reaction centers obtained by this method had an absorbance ratio between 280 and 800 nm that ranged from 1.8 to 2.1 in wild-type reaction centers and from 2.0 to 2.2 in mutant reaction centers. This isolation procedure does not yield reaction centers as pure as can be obtained by other methods (*42*). However, the yield is considerably higher using this technique, and a similar procedure has been employed for a number of mutant reaction centers in *Rb. capsulatus* which are somewhat less stable than wild-type (*35*). Wild-type reaction centers prepared in this way contain the normal complement of bacteriochlorophyll, bacteriopheophytin, and carotenoid, as determined by HPLC analysis of extracts (*43*). However, Q_B is almost completely missing, as assayed by the lifetime of the recombination reaction after a short flash (*44*). Triton X-100-exchanged reaction centers were prepared by ion-exchange chromatography as previously described (*41*).

Ionic Strength, pH, and Detergent Effect Assays. The effect of ionic strength on the steady-state room temperature spectra of wild-type and mutant reaction centers was determined by addition of KCl. Reaction center samples were first diluted to an optical density of approximately 2 in buffer B. 0.5 mL aliquots were then transferred to 1.5 mL microfuge tubes. 0.5 mL of a "2x" KCl solution was then added to the reaction centers to give final concentrations of KCl ranging from 0 to 750 mM. The samples were prepared in this manner so that the optical density would be exactly the same for each sample and no normalization of the plots was necessary. The effect of pH on the steady-state room-temperature spectra was determined with the dilution of reaction centers in either of two buffers, Bis-tris propane (BTP) or 2-amino-2-methyl-1-propanol (AMP). AMP was used to control pH between 6.5 and 9 while BTP was used to control pH between 9 and 11. Reaction center samples were prepared at pH 9 in both buffers to observe any buffer dependent spectral differences. The buffers were prepared such that the same ionic strength (25 mM) was maintained at all pH values from 6.5 to 11. This was done by adding KCl, as needed, to offset the amount of buffer in the uncharged form. In addition to the buffer and KCl, 0.04% Triton X-100 was added to keep the reaction centers in solution.

The effect of ionic detergents on the steady state room temperature spectra was determined with the negatively charged detergent, deoxycholate (DOC), and the positively charged detergent, cetyltrimethylammonium bromide (CTAB). The concentration of each of these detergents was varied from 0.03% to 0.15% in either buffer B or buffer B with 750 mM KCl. Samples were prepared by adding 3 μL aliquots of 10% detergent to 1 mL of reaction centers. Dilution effects were negligible. Spectra were obtained with a Beckman DU64 spectrophotometer from 250 to 900 nm.

Measurement of P/P+ Midpoint Potentials. Electrochemical titration of midpoint potentials was performed in collaboration with Drs. Nagarajan and Parson at the University of Washington in Seattle essentially as described previously (*45*).

Subpicosecond Resolution Transient Absorption Spectroscopy. The femtosecond transient absorption spectrometer has been described previously (*38*, *46*). The fundamental ultrashort pulses were provided by a sychronously pumped, Rhodamine 590 dye laser that was further amplified in a 540 Hz dye amplifier. These pulse trains were split into two beams. Each beam was used to generate a white-light continuum. A spectral region was selected from one of the two continua by passing it through an appropriate interference filter at the desired excitation wavelength and then this was reamplified in a dye amplifier. The other continuum beam was used directly as the source of probe pulses and whole spectra were collected simultaneously using a dual diode array. The polarization of the probe pulses was set at the magic angle with respect to that of the excitation pulses. For all experiments reported, each time scan consisted of 100 spectra at 1 ps intervals, each encompassing a 300-nm region between 700 and 1000 nm. Data were averaged for 2 s (1080 shots) per time point.

To avoid accumulation of the state P^+ in the reaction center samples, a rotating circular sample cell was used as previously described (*38*, *46*). The cuvette had a 3-mm path length and a circumference of 50 cm. It rotated at about 2 Hz. The total sample volume was about 7−8 mL. This rotation rate was rapid enough so that the excited region of the sample was removed completely from the excitation beam between pulses. The pulse energies used in these experiments were approximately 3 μJ/pulse [about 150 μJ/(cm^2 pulse)]. For these experiments, the sample was excited at 820 nm (near the peak of the short-wavelength form of *sym2-1* reaction centers), and the excitation pulses had a spectral width of roughly 5 nm (full width at half-maximum). The long-time absorption changes in the Q_Y band of P were always less than or equal to 20% of the total absorption in that wavelength region. Reduced samples were prepared in 0.05% Triton X-100, 10 mM potassium phosphate buffer (pH 7.8), 300 mM KCl, and 5 mM sodium dithionite.

Temperature Effect Assays. Reaction centers were prepared in buffer B (10 mM potassium phosphate, pH 7.8 with 0.05% LDAO) and mixed with 100% glycerol in a one-third to two-thirds ratio, so that the amount of glycerol in solution was about 67% by volume. Ground-state absorbance spectra of isolated reaction centers were taken from 300 to 1300 nm on a Cary 5 spectrophotometer with a signal averaging time of 0.300 s and a data interval of 1.00 nm. The spectral bandwidth was fixed at 2.00 nm and the detector changeover was set to 900 nm. The difference in absorbance due to the detector changeover was subtracted at 900 nm for each spectrum. The temperature of the sample was controlled between 290 and 10 K using a helium displex refrigeration unit monitored by a thermocouple (APD). The samples were cooled to 10 K in an optical cell with a 2 mm path length. Measurements were taken as the samples warmed from 10 K to room temperature because it was found that the spectra were less likely to become distorted by changes in sample cracking during an increase in temperature. A region of the 10 K glassy sample free of cracks was placed in the light beam and then the temperature was increased in steps. The sample was allowed to equilibrate at each temperature for 10 min before spectra were taken. Air was used as the reference for these measurements.

RESULTS

Description of the Mutation. The *sym2-1* mutation was constructed as part of a set of symmetry mutants in which sections of the M subunit were replaced by the analogous regions of the quasi-symmetrically related L-subunit (*37*). Figure 1 shows the detailed changes between the wild-type and *sym2-1 puf* M gene product and indicates which amino acids come in close contact with which reaction center cofactors. Among the mutated amino acids are residues that come in close contact with P, B_A, and H_A. Figure 1 also shows a representation of the structure of the *Rb. sphaeroides* reaction center L and M sequences, which are homologous to the *Rb. capsulatus* sequences replaced in this mutant. In addition, the relative positions and orientations of the pigments are shown (*1*). This mutation involves replacing a segment in the upper part of the D helix of the M-subunit with that from the L-subunit. Homology between the primary amino acid sequences of *Rb. capsulatus* and *Rb. sphaeroides* is very high (≥80%) in this region. Thus, the *Rb. sphaeroides* structure near P is likely a reasonable model for structural comparison with *Rb. capsulatus*.

Ionic Strength Dependence of the Q_Y Band of P. Reaction centers from *sym2-1* freshly eluted after solubilization and purification on an ion-exchange column in approximately 350 mM KCl showed a peak absorbance for the Q_Y transition of P at about 852 nm, essentially the same as wild-type (Figure 2, upper panel). However, after these reaction centers were dialyzed against buffer B (10 mM potassium phosphate, pH 7.8, with 0.05% LDAO) with no KCl, the Q_Y transition of P was near 820 nm and appeared as a shoulder on the 802 nm monomer bacteriochlorophyll transition (the 0 mM KCl spectrum is essentially the same as the 30 mM KCl spectrum shown in the middle panel of Figure 2).

If KCl was quickly added back after a brief dialysis, almost complete reversibility of the spectral shift could be achieved (data not shown). However, if the dialyzed sample was stored at low salt for extended periods (even frozen), only partial reversibility could be achieved. Figure 2 shows a detailed analysis of the ionic strength dependence of the spectrum of the Q_Y band of P in reaction centers that had been stored in buffer B without additional KCl at −80 °C after dialysis. When reaction centers of *sym2-1* were subjected to incrementally increasing amounts of KCl, the Q_Y band of P changed from the short-wavelength, low-salt form in the absence of any added KCl, to a mixture of the 820 and 850 nm forms in the presence of 750 mM KCl (Figure 2). The overlaid *sym2-1* spectra reveal an isobestic point at 845 nm. The spectra are essentially unaltered with varying ionic strength in regions other than the 800−860 nm region. The ground-state spectrum of the Q_Y transition of P in wild-type reaction centers could also be altered by changing the ionic strength, but to a smaller extent. The wild-type spectral shift is only obvious at the very highest ionic strengths, near 750 mM. The overlaid spectra of wild-type reaction centers at different ionic strengths reveal an isobestic point at 860 nm.

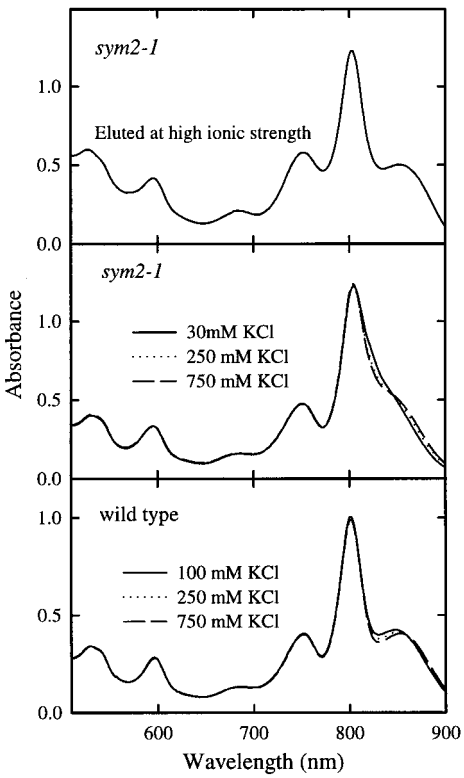

FIGURE 2: Ground-state absorption spectra of mutant and wild-type *Rb. capsulatus* reaction centers as a function of ionic strength. The overlaid spectra in this figure were not normalized. Samples were prepared by a 1/2 dilution of reaction centers in varying amounts of KCl in buffer B. The stock sample of reaction centers for the bottom two panels was a dialyzed sample that was previously frozen. The top panel shows spectra for a reaction center sample taken directly after elution from a preparative column at high ionic strength.

Detergent Effects on the Ground-State Absorbance Spectrum of sym2-1. Adding ionic detergents to the *sym2-1* mutant reaction centers resulted in a much more complete shift between the two spectral forms of P, even after extended storage of reaction centers at low ionic strength. Figure 3 shows the spectral effects observed in both *sym2-1* and wild-type reaction centers as a function of the addition of charged detergents. As with ionic strength effects, the only region of the reaction center spectrum significantly affected is the

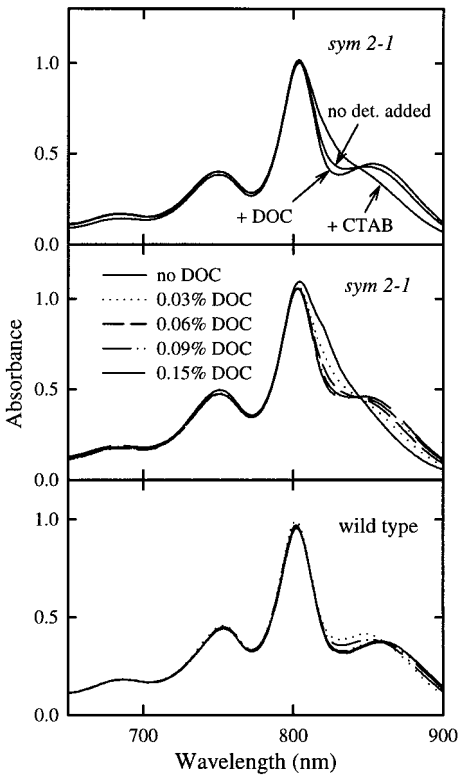

FIGURE 3: Top panel of the figure shows the ground-state absorption spectra of *sym2-1* reaction centers in the presence 0.03% of either a negatively charged detergent, deoxycholate (DOC) or a positively charged detergent, N,N-dimethyl-dodecylamine-*N*-oxide (CTAB) compared to a sample in the absence of these charged detergents. Reaction centers were prepared in buffer B and 750 mM KCl. The center panel in this figure shows dialyzed *sym2-1* reaction centers in buffer B after addition of various concentrations of DOC. The bottom panel is the same as the center panel except using wild-type reaction centers. The DOC concentrations and line types in the lower panel are as given for the middle panel. No normalization was applied to the spectral traces shown in any of the figure panels. Detergents were added by 3 μL additions from 10% stock solutions to 1 mL of sample in a glass cuvette.

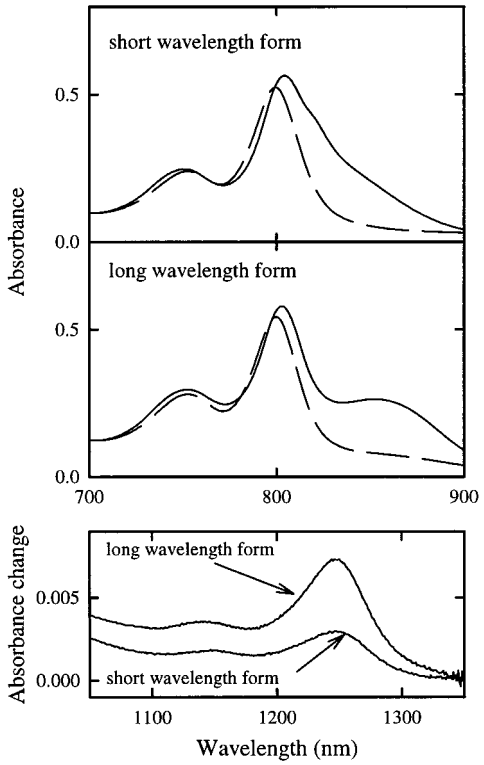

FIGURE 4: Top two panels show the light (photobleached, dashed line) and dark (ground state, solid line) room-temperature absorbance spectra of *sym2-1* reaction centers. Reaction centers were either dialyzed to buffer B with no added KCl to obtain the short-wavelength form, or freshly purified, undialyzed reaction centers were used for the long-wavelength form. The bottom portion of the figure shows light-minus-dark difference spectra from 1000 to 1350 nm obtained on a Cary 5 spectrophotometer. The P^+ band is at 1250 nm.

800−860 nm region. Previous studies have shown that the position of the P band in isolated reaction centers from wild-type *Rb. capsulatus* is dependent on the nature of detergent present in the sample (*26*). The peak of the wild-type Q_Y transition of P shifts from 858 to 848 nm in the presence of CTAB (Figure 3, bottom panel). The detergent effect is much more pronounced in the *sym2-1* mutant reaction centers, where the peak shifts from 853 nm in the presence of high salt and the negatively charged detergent, deoxycholate (DOC), to about 820 nm in the presence of the positively charged detergent, cetyltrimethylammonium bromide (CTAB) (Figure 3, upper panel). Apparently, the charge of the detergent, to a great extent, is dominant over any effects of ionic strength. For example, in the presence of 750 mM KCl, the addition of CTAB to a final concentration of 0.03% resulted in a *sym2-1* steady-state spectrum essentially identical to the dialyzed *sym2-1* ground-state spectrum at low KCl concentration (compare Figures 2 and 3). The addition of incremental amounts of detergent to isolated *sym2-1* reaction centers again revealed an isobestic point at 845 nm for *sym2-1* reaction centers and an isobestic point at 860 nm for isolated wild-type reaction centers (Figure 3).

pH Effects on the Ground-State Absorbance Spectrum of sym2-1. Compared to the ionic strength and detergent effects, no significant effects on the ground-state spectrum were observed when *sym2-1* reaction centers were subjected to pH values ranging from 6.5 to 10.95 as described in Materials and Methods. A small degradation of sample was noted at the highest pH values of 10.5 and 10.95 for both wild-type and *sym2-1* reaction centers (not shown).

Photobleaching Spectra. The top portion of Figure 4 shows dark and photobleached spectra of *sym2-1* in both the 852 nm (long wavelength) and 820 nm (short wavelength) forms. The long-wavelength form was obtained from reaction centers taken directly after chromatographic purification and elution in high salt from a DEAE column. The short-wavelength form was obtained upon dialysis of the long-wavelength reaction centers in buffer B. The photobleached spectra of both forms are nearly identical.

The bottom portion of Figure 4 shows the light minus dark difference spectra of *sym2-1* in both the 853 and 820 nm forms in the spectral region where P^+ absorbs near 1250 nm. The oscillator strength of the P^+ difference absorbance band near 1250 nm decreases by more than a factor of 2 in the long-wavelength form relative to the short-wavelength form in both wild-type (not shown) and mutant reaction centers.

P/P+ Midpoint Potentials as a Function of Ionic Strength. Table 1 reports the P/P+ midpoint potential of reaction centers isolated from wild-type and *sym2-1* reaction centers at both high and low ionic strength**.** These measurements were performed by monitoring the bleaching of the Q_Y

Table 1: P/P+ Midpoint Potentials[a]

sample	E_m (mV)[b]	n[c]
wild type in buffer B and 20 mM KCl	270	1.045
wild type in buffer B and 280 mM KCl	274	1.066
sym2-1 in buffer B and 20 mM KCl	288	0.97
sym2-1 in buffer B and 280 mM KCl	318	1.006

[a] This analysis was done using electrochemical methods. [b] The potentials are measured versus the Ag/AgCl electrode. [c] n is the factor in the Nernst equation (used to fit the electrochemical oxidation curve) which denotes the number of electrons involved in the reduction/oxidation reaction. The statistical error in the data is about ±10 mV.

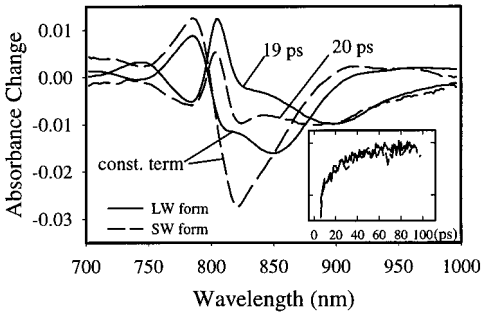

FIGURE 5: Amplitude spectra resulting from a global fit of a time/wavelength surface covering 100 ps of time and 300 nm of wavelength for both the short and long-wavelength forms of the reaction center. The fits were to an exponential and a constant term. The exponential term had a rate constant of 19 ps for the long-wavelength form (solid line) and 20 ps for the short-wavelength form (dashed line). The inset shows the decay of the stimulated emission from the two forms of the reaction centers at 908 nm (long-wavelength form, solid line) and 888 nm (short-wavelength form, dashed line).

transition of P from 800 to 850 nm while changing the ambient potential with an electrochemical cell (*45*). The electrochemical titrations were performed in collaboration with Drs. Nagarajan and Parson at the University of Washington. The long-wavelength form of the *sym2-1* mutant had a P/P+ midpoint potential nearly 50 mV higher than the long-wavelength form of wild-type. Upon dialysis, the midpoint potential of the mutant dropped by 30 mV. In contrast, wild-type reaction centers showed essentially no difference in the P/P+ midpoint point potentials of the long- and short-wavelength forms of the reaction center.

Initial Electron-Transfer Rate in the Two Different Reaction Center Spectral Forms. Room-temperature subpicosecond resolution transient absorbance measurements of *sym2-1* reaction centers were obtained for both reaction centers in predominantly the long wavelength and short-wavelength forms. Figure 5 shows the amplitude spectra resulting from a global fit of a time/wavelength surface covering 100 ps of time and 300 nm of wavelength for both forms using the equation $A_1\exp(-k_1t)$ + const. The time constants for P* decay (and thus presumably the initial electron transfer event) were essentially the same in the two forms (20 and 19 ps for the short and long-wavelength forms, respectively). Similar measurements on wild-type reaction centers have also shown no difference in initial electron-transfer kinetics between the short- and long-wavelength forms (*26*). Looking at the constant term in the amplitude spectrum (which is essentially the difference absorbance spectrum of $P^+H_A^-$), it is clear that the spectral form of P that was bleached in the two samples was quite different, with the short-wavelength form showing the greatest bleaching at 820 nm

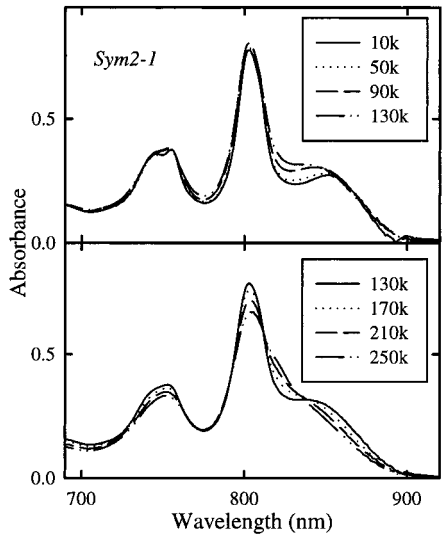

FIGURE 6: Ground-state absorption spectra of *sym2-1* reaction centers as a function of temperature between 10−130 K (top panel) and 130−210 K (lower panel). The reaction centers were prepared in the short-wavelength form at room temperature by dialysis into buffer B with no salt. Glycerol was then added as a cryoprotectant (2:1 v:v glycerol to buffered sample).

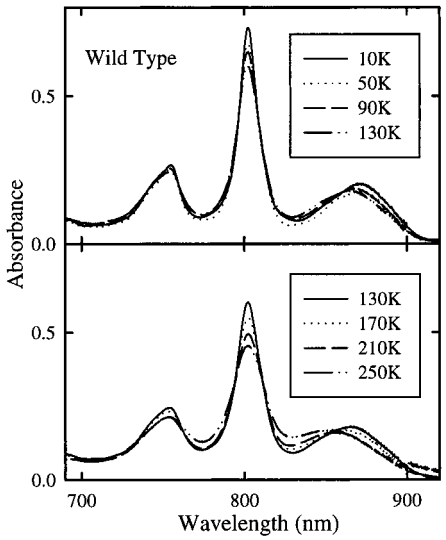

FIGURE 7: Ground-state absorption spectra of wild-type *Rb. capsulatus* reaction centers as a function of temperature between 10−130 K (top panel) and 130−210 K (lower panel). The reaction centers were prepared as in Figure 6.

and the long-wavelength form at 850 nm. The spectra of the 19 or 20 ps components of the amplitude spectra also differ. There is clearly a larger initial absorbance recovery in the 800−850 nm region in the short-wavelength form of the mutant than in the long-wavelength form. This appears to be partially due to a broadening and blueshift of the stimulated emission and partially due to some ground-state recovery at 820 nm.

Temperature Dependence of the Ground-State Absorbance Spectrum. Figures 6 and 7 show ground-state absorbance measurements of *sym2-1* and wild-type reaction centers which had been dialyzed into buffer B with no added KCl before mixing with glycerol. As described in the Materials and Methods, dialysis of *sym2-1* reaction centers at low ionic strength results almost entirely in a reaction center conformation in which the peak of the near-infrared absorbance band

of the donor, P, is shifted to 820 nm, compared to 850 nm directly upon isolation at high ionic strength. For the measurements in Figures 6 and 7, the temperature was controlled by a helium displex refrigerator (see Materials and Methods) from 250 to 10 K. Spectra at 10 K were essentially the same as those previously described (*38*) for *sym2-1* reaction centers at 20 K, though the previous measurements were performed in a Triton X-100-containing buffer, rather than in LDAO. This apparently has little effect on the low-temperature spectra of the reaction center samples. Figure 6 (upper panel) shows a series of spectra taken as *sym2-1* reaction centers were warmed from 10 to 130 K. Over this temperature range, the peak of the P band absorbance shifted from 855 nm at 10 K to 850 nm at 130 K. During this temperature increase, a broadening of the long-wavelength absorbance band was also observed. There is very little change between 10 and 130 K in the 800 nm absorbance band.

When *sym2-1* reaction centers were warmed from 130 to 250 K (Figure 6, lower panel), the absorbance near 850 nm decreased and the absorbance near 820 nm increased, revealing a nearly isobestic point at about 838 nm. Note that no isobestic point was observed for temperature changes below 130 K. For comparison, similar measurements are shown in Figure 7 for wild-type reaction centers. The results for wild-type are similar to the *sym2-1* mutant, except less pronounced. The overlaid spectra show the Q_Y transition of P in the wild-type broadening as the temperature is increased and shifting from a peak maximum at 875 nm at 10 K to 865 nm at 130 K with no clear isobestic point. As the wild-type reaction centers were warmed further from 130 to 250 K, the absorbance at 865 nm decreased and absorbance to the blue increased showing a nearly isobestic point near 855 nm for wild-type reaction centers (Figure 7, lower panel).

DISCUSSION

It has been known for some time that there are at least two distinct conformations of the bacterial reaction center with spectral differences in the Q_Y band of P (*23*−*32*, *47*). The specific effects of ionic detergents have been discussed in some detail by Wang et al. (*26*) and Muh et al. (*28*) for wild-type *Rb. capsulatus* reaction centers. In wild-type, there is a roughly 15 nm shift between the blue absorbing form observed in the presence of cationic detergent and the red absorbing form which is found in the presence of neutral or anionic detergents (*26*). ENDOR measurements of P^+ reveal that two distinct forms are all that are required to describe the hyperfine coupling data obtained for reaction centers in the presence of different detergents, different ratios of detergent to reaction center or varying temperatures (*28*). There are significant differences in unpaired spin densities between the two forms (*28*). These observations were explained in terms of changes in the energy difference between the HOMOs of the two halves of the bacteriochlorophyll dimer and changes in the resonance integral (orbital overlap) between the two bacteriochlorophylls that make up the dimer. It was concluded that the observed hyperfine couplings were most consistent with small changes in the relative orientations of the two halves of the dimer upon changing detergents, rather than, for example, changes in the position of the ring I acetyl group which is known to shift the spectrum.

Two-State Conformational Equilibrium Model. The present work focuses on a mutant which shows the same types of responses of its optical spectrum to ionic detergents that have been observed previously in wild-type reaction centers, except that the spectral shift between forms is considerably more pronounced (about 30 nm, Figure 3). The similar behavior observed in the spectrum of reaction centers from this mutant upon changing the ionic strength (Figure 2), nature of the detergent (Figure 3), and temperature (Figure 6), suggests that these processes have the same underlying mechanism in the mutant as in wild-type. The fact that an identifiable isobestic point is present in each case suggests that all of these processes can be described in terms of a shift in equilibrium between two distinct spectral forms of the reaction center. This isobestic point is not as obvious in wild-type, but can be seen by comparison and is at 860 nm. This two-state approach is very similar to that taken by Muh et al. in the analysis of the ENDOR data taken on the two spectral forms observed for wild-type (*28*) and will be the basis for the remainder of the analysis.

Ionic Strength Alone Is Not Sufficient To Convert the Reaction Center between the Short- and Long-Wavelength Forms. The ionic strength effect on the spectrum of *sym2-1* seems to be dependent on how the sample is prepared. Upon extensive dialysis at low ionic strength, adding salt back is not enough to cause a complete shift to the long-wavelength form (Figure 2). Similarly, reaction centers frozen at low ionic strength in the absence of cryoprotectants cannot be shifted back to the long-wavelength form with salt alone [this has also been observed for wild-type (*28*)]. Switching detergents, however, will cause a complete shift under either of these conditions (Figure 3). This suggests that the ionic strength effect on the equilibrium between the two forms is sensitive to other components that are lost during extensive dialysis or upon freezing, while the detergent effect is not (perhaps bound ionic lipid molecules are lost during dialysis or freezing which can be replaced by the ionic detergent molecules). For the analysis of the spectral properties of the two forms given below, care was taken to use samples as completely driven into one spectral form of the mutant or the other as possible.

Additional Spectral Properties of the Two Conformational Forms of the Reaction Center at Room Temperature. Upon photooxidation of P, the spectrum of the reaction centers in the two forms is essentially identical, implying that the conformational change affects only the P transition (Figure 4). This is consistent with the work of Parson and Warshel (*48*), whose theoretical calculations suggest that (at least in *Rhodobacter viridis*) the lowest excited state of P would be much more sensitive to changes in the energy of charge transfer bands of P (which in turn should be sensitive to the electrostatic nature of the environment) than would other transitions in the reaction center. As has been seen previously in wild-type (*26*, *28*), the 1250 nm P^+ transition loses substantial intensity upon conversion from the long- to the short-wavelength form (Figure 4). The possible reasons for this have been discussed by Muh et al. (*28*). Note that the 1250 nm transitions shown in Figure 4 were obtained by comparing freshly prepared reaction centers just off the column in high ionic strength to dialyzed reaction centers in low ionic strength buffer. This gives the same oscillator strength changes that Muh et al. (*28*), have seen in wild-

type in the presence of different ionic detergents and that they have correlated with the changes in the ENDOR spectrum. This gives additional evidence that all of these observables (ionic strength effects, detergent effects, and the ENDOR spectral changes) have a common origin.

Electron-Transfer Kinetics in the Long- and Short-Wavelength Forms of the Reaction Center. The larger spectral difference between the two forms of the reaction center has made it possible to perform fast transient absorbance measurements in which the spectral signatures of the two forms are much more distinct than that seen previously with wild-type (*26*). The amplitude spectra of the constant components in Figure 5 represent the difference absorbance spectrum of the charge-separated state $P^+H_A^-$ in each of the two spectral forms (for these experiments, electron transfer to the quinone was blocked by quinone reduction). One might be concerned that excitation at 820 nm would only excite the 820 nm form of the reaction center, regardless of the sample conditions. However, it is clear from Figure 5 that under buffer conditions where predominantly the long-wavelength spectral form of the reaction centers is present, the 850 nm band has been bleached, implying that it is the long-wavelength form of P that is predominantly undergoing electron transfer under these conditions. Similarly, under buffer conditions that give rise predominantly to the short-wavelength form, the main bleaching band is at 820 nm, implying that it is the 820 nm form of P that is predominantly undergoing photochemistry in this sample.

As shown in the inset to Figure 5, the kinetics of the decay of the stimulated emission are essentially identical in the two forms of the *sym2-1* reaction center, giving decay time constants of 19 and 20 ps for the long- and short-wavelength forms, respectively. The spectrum of the stimulated emission can be seen in the 19 and 20 ps component amplitude spectra of Figure 5 near 900 nm. The stimulated emission spectrum appears broader and somewhat blueshifted in the short-wavelength form of the reaction center compared to the long-wavelength form. The breadth may indicate that even after dialysis at low ionic strength there is a minority contribution from the long-wavelength form to the spectrum. This is consistent with the absorbance spectrum (Figure 2) and the difference spectrum of the charge-separated state (the constant amplitude spectrum of Figure 5 for the short-wavelength form), which both show some contribution in the 850 nm region where the long-wavelength form absorbs.

Comparison of the 19 and 20 ps component amplitude spectra of Figure 5 also suggests that there is some ground-state recovery near 820 nm in the short-wavelength form. This implies that the yield of electron transfer from the 820 nm form may not be unity, presumably because some relatively fast decay path has been introduced by the spectral shift that is not present in wild-type or the long-wavelength form. If we assume that all of the negative bleaching in the 820 nm region is due to yield loss (looking at the 20 ps amplitude spectrum of Figure 5), then the yield of initial charge separation in the short-wavelength form would be about 75%. Very likely some of the bleaching decay is actually decay of stimulated emission extending farther to the blue in this spectral form of the mutant than in the long-wavelength form, giving an artificially low apparent yield of charge separation for the short-wavelength form in the mutant (a true yield of 85% would be a good estimate based on the overall shapes of the spectra). Because the yield of charge separation in the short-wavelength form is not 100%, the observed charge separation time for this form may be somewhat faster than the microscopic time constant for charge separation (which might be as slow as 25 ps). However, this is a small correction that does not significantly affect the conclusion that the electron-transfer rates are very similar in the two spectral forms of the mutant.

It is noteworthy that a shift in the absorbance transition energy of P by roughly 50 meV (30 nm in this region of the spectrum) has very little effect on the overall kinetics of initial electron transfer. The 50 meV P* energy increase in the short-wavelength form of *sym2-1* reaction centers is accompanied by a 30 mV decrease in the P/P^+ midpoint potential compared to the long-wavelength form (Table 1). Thus, the change in the overall driving force for charge separation between the two forms of the reaction center is presumably on the order of 80 meV (ignoring relaxation processes). The insensitivity of the electron-transfer rate to this change is consistent with past results that have shown that increasing the driving force for electron transfer by about this amount has very little effect on the electron-transfer rate (*49*). The similarity of electron transfer times between the two forms also suggests that whatever the nature of the conformational change between these forms is, the relative distances and orientations of the cofactors involved in the initial electron transfer reaction are not greatly altered.

Temperature Dependence of the Ground-State Absorbance Spectrum. Figures 6 and 7 show that a similar shift between two spectral forms of the reaction center is observed as the temperature is changed from 130 to 250 K. In fact, for both the *sym2-1* and wild-type reaction centers, the isobestic points observed in the temperature dependence above 130 K are similar to those observed at room temperature upon varying salt and detergent (838 vs 845 nm for *sym2-1* reaction centers and 855 vs 860 nm for wild-type reaction centers). The difference in the isobestic points seen in detergent and ionic strength studies at room temperature vs the temperature dependence studies likely arises from the glycerol solvent environment used for the temperature-dependence studies and the fact that there are probably temperature effects on the spectrum in addition to varying the relative populations of the two spectral conformations. Below 130 K, the conformational interconversion appears to be complete and other effects dominate the temperature dependence of the absorbance band at lower temperatures. The lower end of the glass transition in the glycerol buffer is at roughly 130 K. This is significant, because it is in this temperature range that movement of the solvent largely ceases and, below this point, large-scale changes in the protein structure that involve movement of the surrounding solvent would be frozen out.

The temperature dependence can be analyzed using a simple two-state model, consistent with the past analysis of the two spectral forms of P (*23*−*28*). In a two-conformation system, there should a free-energy difference between the two spectral conformations given by

$$\Delta G = \Delta H - T\Delta S$$

where ΔH is the change in enthalpy, ΔS is the entropy change, and T is temperature. If the entropy and enthalpy

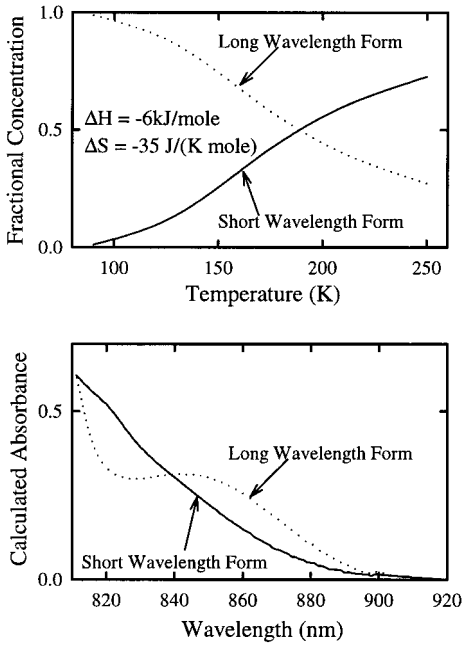

FIGURE 8: Fitting of the temperature-dependent spectra of *sym2-1* reaction centers to a thermodynamic model (see text) resulted in a temperature dependent change in the relative fractional concentrations of the two reaction center spectral conformations (top panel). This could be interpreted in terms of a negative enthalpy and entropy change for formation of the long-wavelength form of the reaction center from the short-wavelength form. The basis spectra of the pure short wavelength and pure long-wavelength form that resulted from the fit are also shown (lower panel).

differences both have the same sign, they will play against each other. In this case, either changes in the environment or changes in the temperature can reverse the sign of the free-energy difference between conformational forms, switching which form has the dominant population.

Using this model, the temperature dependence implies that the longer wavelength form has the more favorable enthalpy, but the less favorable entropy. Figure 8 shows the enthalpy and entropy values that result from fitting the temperature dependence of the *sym2-1* reaction center ground state spectra between 810 and 950 nm taken at five temperatures evenly spaced between 90 and 250 K (data from Figure 6). The fitting function was derived assuming that there were two distinct spectral forms whose relative equilibrium populations depended on the temperature as dictated by

$$A_{tot} = A_S F_S + A_L F_L$$

$$K_{EQ} = \frac{F_L}{F_S} = e^{(-\Delta H + T\Delta S)/RT}$$

Here A_S and A_L are the absorbance spectra of the pure short and long-wavelength forms of the reaction center respectively and F_S and F_L are the fractional amounts of each form at any particular temperature, T. A_{tot} is the total absorbance of the sample, and K_{EQ} is the equilibrium constant for the conformational interconversion between the short- and long-wavelength forms of the reaction center (written in that direction). Solving the second equation for F_S and F_L (by noting that $F_S + F_L$ is 1.0) and substituting into the first equation gives

$$A_{tot} = A_S \frac{1}{1 + e^{(-\Delta H + T\Delta S)/RT}} + A_L \frac{e^{(-\Delta H + T\Delta S)/RT}}{1 + e^{(-\Delta H + T\Delta S)/RT}}$$

Note that for the fitting it is assumed that the two basis spectra, A_S and A_L, are temperature independent. This is almost certainly not strictly true, but over the wavelength range (which excludes the 800 nm band) and temperature range considered, it should be approximately correct. The values of A_S and A_L are allowed to vary separately at each wavelength and thus the basis spectra are parameters of the fit, as are the enthalpy and entropy changes. The fit was constrained to generate only physically reasonable spectra (no negative absorbance values), and the spectra at the endpoints of the temperature range were used as initial guesses for the pure spectra of the long- and short-wavelength forms of the reaction center. The initial guesses are important. If one, for example, enters zeros or ones for the initial absorbance spectra and lets the optimization proceed from there, the system quickly generates physically meaningless spectra with negative regions.

The value of the enthalpy change for the conformational interconversion obtained from the fit of the *sym2-1* data was about −6000 J/mol and the value of the entropy change was −35 J/(K mol). It is important to note that these specific values of the thermodynamic parameters are presumably environment dependent and were determined under conditions (reaction centers dialyzed at low ionic strength), which result in almost completely the short-wavelength form at room temperature. The quality of the fit is very good, with the predicted total spectra being essentially indistinguishable (within a few percent) from the measured spectra of Figure 6 between 810 and 950 nm (if the fit was plotted on top of the data in Figure 6, the fit and data lines would be indistinguishable). It is important to note, however, that values of the entropy and entropy changes within 50% of those given (if appropriately balanced against one another), can also give excellent fits. Outside that range, one of the two basis spectra must have a negative value for an adequate fit to be achieved. This uncertainty in the entropy and enthalpy change values comes from the fact that the basis spectra are not accurately known and varying them provides substantial latitude in the fit.

Fits for the wild-type data were also performed, although the changes were less pronounced. If the fit was performed using the same entropy and enthalpy values determined for *sym2-1* reaction centers, a good fit was obtained, though not as good as the *sym2-1* reaction center fit. Allowing the entropy and enthalpy to vary freely for the wild-type data (with the constraint of physically meaningful basis absorbance spectra) resulted in an enthalpy value about 25% lower and an entropy value roughly a factor of 2 lower than that determined for *sym2-1* reaction centers. The smaller changes observed in the wild-type temperature dependence made the fitting more difficult and the values derived less reliable, but within a factor of 2, which is about the limit of accuracy due to the lack of experimentally determined basis spectra, the *sym2-1* and wild-type reaction center temperature dependence yield similar values for the enthalpy and entropy of conformational interconversion.

The enthalpy and entropy values determined in Figure 8 imply that the longer wavelength form of the reaction center

is a more constrained structure than the shorter wavelength form (either in terms of protein or solvent mobility), but one that involves a larger number of ionized or polar groups interacting with one another or with the solvent. Thus, the free energy of the longer wavelength form would be sensitive to the ionic strength of the surrounding solvent and to the charges on closely associated charged detergent molecules, as observed.

Conformational Difference between the 820 and 850 nm Forms. This raises the question of just what the conformational change is that occurs between the 820 and 850 nm forms of the reaction center. A complete answer to this question is not yet available, but several points can be made from the information presented here in conjunction with previous studies. One obvious possibility for the cause of a large spectral shift in P is the movement of the ring I acetyl group on P [discussed by Muh et al. (*28*)]. However, this seems unlikely both because the expected changes in the spin distribution were not observed (*28*) and because the changes observed in the midpoint potential of P between the two spectral forms of the reaction center are small (Table 1). Mutations known to affect the position of the acetyl group have large effects on both the transition energy of P and its midpoint potential. A case in point is the mutant HF(L168) (*49*). This mutant involves removal of a hydrogen bond to the acetyl group of the A-side bacteriochlorophyll of P and shows a 15 nm blueshift in the peak of the P absorbance band at room temperature. However, this change also results in a large decrease in the midpoint potential of P (about 80 mV). Changing the detergent or ionic environment of the *sym2-1* mutation results in a 30 nm blueshift in the P transition but only a 30 mV decrease in the oxidation potential. In wild-type, a 10−15 nm blueshift is observed between the two spectral forms, but essentially no change in midpoint potential is measured. These observations, combined with arguments based on previous ENDOR measurements of the two spectral forms in wild-type (*28*) make a shift in the acetyl group seem less likely than other possibilities as the primary explanation for the spectral shift between the two forms.

The fact that the conformational change between the two spectral forms of the reaction center results in only a moderate change in the midpoint potential of P in the *sym2-1* mutant and no change in wild-type is interesting (Table 1). This presumably means that generating a formal charge on P (via oxidation) does not very strongly favor either the long- or short-wavelength form of the reaction center. The lack of pH sensitivity in the conformational equilibrium also implies that protonation or deprotonation of reaction center residues does not substantially change the relative energies of the two conformational forms (at least rapidly protonatable groups). Thus, the change between the two forms of the reaction center probably is not due to protonation of accessible amino acids.

Muh et al. suggested that a change in the relative geometry of the bacteriochlorophylls in P might be the cause of the spectral shift upon changing from positively to negatively charged detergents in wild-type reaction centers (*28*). One might expect that such a shift would also change the orbital overlap with neighboring acceptor molecules and thus affect the electron-transfer rate. However, no significant difference in the initial electron-transfer kinetics is seen in either the *sym2-1* mutant or wild-type (ref *26*, Figure 5) between the long- and short-wavelength forms of the reaction center. It is possible that a small geometric change in P occurs. The work of Parson et al. has shown by theoretical calculations that a small change in the geometry of P can lead to large spectral changes (*48*). If changes in orientation are responsible for the spectral shifts, these changes must be along dimensions that do not significantly alter the coupling between electron transfer components in the system, because electron transfer rates do not vary substantially between spectral forms (Figure 5).

Previous work on bacterial light harvesting systems suggests another possibility. In light harvesting systems, a change in hydrogen bonding to the bacteriochlorophyll is attributed to a spectral change from 850 to 820 nm (*50*−*57*). It is conceivable that there exists some kind of hydrogen-bonding change occurring in *sym2-1* reaction centers with detergent, ionic strength and temperature. However, mutants which introduce or remove hydrogen bonds to P have been shown to shift the position of the P band by only 10−15 nm, a considerably more modest change than observed here (*49*).

Another possible explanation for the shift between the long- and short-wavelength forms of the reaction center is a more direct effect on the local electric field in the vicinity of P. This could be due to a charge interaction between some charged molecule (detergent, phospholipid, or buffer ion) and P itself or it could be indirect via changes in the hydration of the protein, which would alter the effective dielectric constant. It is interesting that in this respect, at least in wild-type at low temperature, the addition of glycerol seems to favor formation of the long-wavelength form of the reaction center (*28*). Glycerol tends to dehydrate proteins and their surroundings. High ionic strength may also cause dehydration and thus a shift toward the long-wavelength form. Thus, one possible mechanism of the shift from the long to short-wavelength forms of the reaction center could be changes in the effective field felt by the special pair because of changes in hydration state and/or surface charge (which would be sensitive to ionic detergents). If the long-wavelength form involves a larger number of ionic interactions, then changes in hydration may result in a more constrained structure for the water both within and around the reaction center or perhaps less water within the reaction center as the conformation closes up to allow more direct interactions between polar groups in the protein. This would presumably be a more enthalpically favored form of the system, but would have an entropic cost, as the positions of the water molecules, and/or the protein residues, would be more constrained.

Hydration effects on conformational changes have been observed in a number of other proteins. For example, changes in hydration accompany the reduction of cytochrome oxidase (*58*) and the binding of oxygen to hemoglobin (*59*). Studies on yeast hexokinase binding to its substrate glucose in solution have shown that changes in the hydration state of the protein bring about changes in conformation that affect substrate binding (*60*). There is also evidence for a controlling role of water in producing the native bacteriorhodopsin structure (*61*). The nonnative bacteriorhodopsin structure exhibits altered spectral and kinetic properties of its photocycle. Bacteriorhodopsin mutants have been made that affect

the ability of bacteriorhodopsin to form appropriate water structures in specific protein cavities, destabilizing the native form of the protein (*61*).

In the reaction center itself, calculations of the effects of protein relaxation on the dielectric constant in *Rb. sphaeroides* reaction centers have shown that the effective dielectric constant of the protein is in part determined by the degree of water penetration in the protein (*62*). In addition, past studies of reaction centers in poly(vinyl alcohol) films have shown that hydration has significant spectral effects (*5*, *63*, *64*).

CONCLUSIONS

The enhanced differences between the spectral forms of the long-wavelength P transition in *sym*2−1 reaction centers have made a detailed analysis possible of both the properties of these two reaction center spectral forms and the thermodynamics of interconversion between them. The two forms are functionally similar, undergoing electron transfer with similar time constants. Thus, largely different transition energies of the initial electron donor have relatively little effect on the overall charge separation reaction. In addition, much of the temperature dependence in the 130 to 295 K temperature range can be described in terms of a temperature-dependent equilibration between these two forms, giving rise to an enthalpy change for the interconversion of −6000 J/mol and an entropy change of −35 J/(K mol). Similar thermodynamic parameters can be used to describe the less pronounced spectral changes with temperature in wild-type.

ACKNOWLEDGMENT

The authors would like to thank Drs. William Parson and V. Nagarajan for assisting us with potentiometric titrations that were performed in their laboratory and also for helpful discussions. Drs. James Allen and JoAnn Williams are also acknowledged for insightful comments. This is publication no. 441 from the Arizona State University Center for the Study of Early Events in Photosynthesis.

REFERENCES

1. Allen, J. P., Feher, G., Yeates, T. O., Komiya, H., and Rees, D. C. (1987) *Proc. Natl. Acad. Sci. U.S.A. 84*, 6162−6166.
2. Chang, C.-H., El-Kabbani, O., Tiede, D., Norris, J., and Schiffer, M. (1991) *Biochemistry 30*, 5352−5360.
3. Ermler, U., Fritzsch, G., Buchanan, S. K., and Michel, H. (1994) *Structure 2*, 925−936.
4. Lancaster, C. R. D., Ermler, U., and Michel, H. (1995) in *Anoxygenic Photosynthetic Bacteria* (Blankenship, R. E., Madigan, M. T., and Bauer, C. E., Eds.) pp 503−526, Kluwer Academic Publishers, Netherlands.
5. Okamura, M. Y., Feher, G., and Nelson, N. (1982) in *Photosynthesis: Energy Conservation by Plants and Bacteria* (Govindjee, Ed.) pp 195−229, Academic Press, New York.
6. Kirmaier, C., and Holten, D. (1987) *Photosynth. Res. 13*, 225−260.
7. Zinth, W., and Kaiser, W. (1993) in *The Photosynthetic Reaction Center* (Deisenhofer, J., and Norris, J. R., Eds.) pp 71−88, Academic Press, San Diego.
8. Kirmaier, C., and Holten, D. (1993) in *The Photosynthetic Reaction Center* (Deisenhofer, J., and Norris, J. R., Eds.) pp 49−70, Academic Press, San Diego.
9. Martin, J.-L., and Vos, M. H. (1992) *Annu. Rev. Biophys. Biomol. Struct. 21*, 199−222.
10. Parson, W. W. (1991) in *Chlorophylls* (Scheer, H., Ed.) pp 1153−1180, CRC Press, Boca Raton.
11. Woodbury, N. W., and Allen, J. P. (1995) in *Anoxygenic Photosynthetic Bacteria* (Blankenship, R. E., Madigan, M. T., and Bauer, C. E., Eds.) pp 527−557, Kluwer Academic Publishers, Dordrecht.
12. Parson, W. W. (1996) in *Protein Electron Transfer* (Bendall, S. D., Ed.) pp 125−160, BIOS Scientific Publishers, Oxford.
13. Deisenhofer, J., Epp, O., Huber, R., and Michel, H. (1984) *J. Mol. Biol. 180*, 385−398.
14. Williams, J. C., Steiner, L. A., Ogden, R. C., Simon, M. I., and Feher, G. (1983) *Proc. Natl. Acad Sci. U.S.A. 80*, 6505−6509.
15. Williams, J. C., Steiner, L. A., Feher, G., and Simon, M. I. (1984) *Proc. Natl. Acad. Sci. U.S.A. 81*, 7303−7307.
16. Youvan, D. C., Bylina, E. J., Alberti, M., Begusch, H., and Hearst, J. E. (1984) *Cell 37*, 949−957.
17. Heller, B. A., Holten, D., and Kirmaier, C. (1995) *Science 269*, 940−945.
18. Lin, S., Jackson, J. A., Taguchi, A. K. W., and Woodbury, N. W. (1999) *J. Phys. Chem. B 103*, 4757−4763.
19. Kirmaier, C., Weems, D., and Holten, D. (1999) *Biochemistry 38*, 11516−11530.
20. Katilius, E., Turanchik, T., Lin, S., Taguchi, A. K. W., and Woodbury, N. W. (1999) *J. Phys. Chem. B 103*, 7386-7389.
21. Bylina, E. J., Robles, S. J., and Youvan, D. C. (1988) *Isr. J. Chem. 28*, 73−78.
22. Jones, M. R., Visschers, R. W., and van-Grondelle, R. (1992) *Biochemistry 31*, 4458−65.
23. Mar, T., and Gringas, G. (1995) *Biochemistry 34*, 9071−9078.
24. Clayton, R. K. (1978) *Biochim. Biophys. Acta 504*, 255−264.
25. Debus, R. J., Feher, G., and Okamura, M. Y. (1985) *Biochemistry 24*, 2488−2500.
26. Wang, S., Lin, S., Lin, X., Woodbury, N. W., and Allen, J. P. (1994) *Photosynth. Res. 42*, 203-215.
27. Gast, P., Hemelrijk, P. W., Van Gorkom, H. J., and Hoff, A. J. (1996) *Eur. J. Biochem. 239*, 805−809.
28. Muh, F., Rautter, J., and Lubitz, W. (1997) *Biochemistry 36*, 4155−4162.
29. Rautter, J., Lendzian, F., Lubitz, W., Wang, S., and Allen, J. P. (1994) *Biochemistry 33*, 12077−12084.
30. Reddy, N. R. S., Kolaczkowski, S. V., and Small, G. J. (1993) *Science 260*, 68−71.
31. Kalman, L., and Maroti, P. (1997) *Biochemistry 36*, 15269−15276.
32. Brzezinski, P., and Andreasson, L.-E. (1995) *Biochemistry 34*, 7498−7506.
33. Kleinfeld, D., Okamura, M. Y., and Feher, G. (1984) *Biochim. Biophys. Acta 766*, 126−140.
34. Lous, E. J., and Hoff, A. J. (1986) *Photosynth. Res. 9*, 89−101.
35. Taguchi, A. K. W., Stocker, J. W., Alden, R. G., Causgrove, T. P., Peloquin, J. M., Boxer, S. G., and Woodbury, N. W. (1992) *Biochemistry 31*, 10345−10355.
36. Stocker, J. W., Taguchi, A. K. W., Murchison, H. A., Woodbury, N. W., and Boxer, S. G. (1992) *Biochemistry 31*, 10356−10362.
37. Taguchi, A. K. W., Eastman, J. E., Gallo, D. M. J., Sheagley, E., Xiao, W., and Woodbury, N. W. (1996) *Biochemistry 35*, 3175−3186.
38. Lin, S., Xiao, W., Eastman, J. E., Taguchi, A. K. W., and Woodbury, N. W. (1996) *Biochemistry 35*, 3187−3196.
39. Bylina, E. J., Ismail, S., and Youvan, D. C. (1986) *Plasmid 16*, 175−181.
40. Youvan, D. C., Ismail, S., and Bylina, E. J. (1985) *Gene 38*, 19−31.
41. Xiao, W. (1994) *Energy and Electron Transfer in Rhodobacter capsulatus*, Thesis, Arizona State University, Tempe, AZ.
42. Prince, R. C., and Youvan, D. C. (1987) *Biochim. Biophys. Acta 890*, 286−291.
43. Gallo, D. M. J. (1994) Ph.D. Thesis, Arizona State University, Tempe, AZ.

44. Feher, G., Allen, J. P., Okamura, M. Y., and Rees, D. C. (1989) *Nature 339*, 111−116.
45. Nagarajan, V., Parson, W. W., Davis, D., and Schenck, C. C. (1993) *Biochemistry 32*, 12324−12336.
46. Peloquin, J., Lin, S., Taguchi, A. K. W., and Woodbury, N. W. (1995) *J. Phys. Chem. 99*, 1349−1356.
47. Kalman, L., and Maroti, P. (1994) *Biochemistry 33*, 9237−9244.
48. Parson, W. W., and Warshel, A. (1987) *J. Am. Chem. Soc. 109*, 6152−6163.
49. Allen, J. P., and Williams, J. C. (1995) *J. Bioenerg. Biomembr. 27*, 275−283.
50. Fowler, J. S., Sockalingum, G. D., Robert, B., and Hunter, C. N. (1994) *Biochem. J. 299*, 695−700.
51. Fowler, G. J. S., Visschers, R. W., Grief, G. G., van Grondelle, R., and Hunter, C. N. (1992) *Nature 355*, 848−850.
52. Todd, J. B., Parkes-LoACH, P. S., and Leykam, J. F. (1998) *Biochemistry 37*, 17458−17468.
53. Sturgis, J. N., and Robert, B. (1997) *J. Phys. Chem. B 101*, 7227−7231.
54. Visschers, R. W., Chang, M. C., and Van Mourik, F. (1991) *Biochemistry 30*, 5734−5742.
55. Koolhaas, M. H. C., Frese, R. N., and Fowler, G. J. S. (1998) *Biochemistry 37*, 4693−4698.
56. Koolhaas, M. H. C., Van der Zwan, G., and Frese, R. N. (1997) *J. Phys. Chem. B 101*, 7262−70.
57. Somsen, O. J. G., Chernyak, V., and Frese, R. N. (1998) *J. Phys. Chem. B 102*, 8893−908.
58. Kornblatt, J. A., and Bon-Hoa, G. H. (1990) *Biochemistry 29*, 9370−9376.
59. Columbo, M. F., Rau, D. C., and Parsegian, V. A. (1994) *Proc. Natl. Acad. Sci. U.S.A. 91*, 10517−10520.
60. Reid, C., and Rand, R. P. (1997) *Biophys. J. 72*, 1022−1030.
61. Rousso, I., Friedman, N., Lewis, A., and Sheves, M. (1997) *Biophys. J. 73*, 2081−2089.
62. Sham, Y. Y., Muegge, I., and Warshel, A. (1998) *Biophys. J. 74*, 1744−1753.
63. Franzen, S., Goldstein, R. F., and Boxer, S. G. (1990) *J. Phys. Chem. 94*, 5135−5149.
64. Johnson, S. G., Tang, D., Jankowiak, R., Hayes, J. M., and Small, G. J. (1989) *J. Phys. Chem. 93*, 5953−5957.
65. Michel, H., and Diesenhofer, J. (1988) *Biochemistry 27*, 1−7.
66. Michel, H., and Deisenhofer, J. (1986) *EMBO J. 5*, 2445−2451.
67. Yeates, T. O., Komiya, H., Chirino, A., Rees, D. C., Allen, J. P., and Feher, G. (1988) *Proc. Natl. Acad. Sci. U.S.A. 85*, 7993−7997.
68. El-Kabbani, O., Chang, C.-H., Tiede, D., Norris, J., and Schiffer, M. (1991) *Biochemistry 30*, 5361−5369.

BI0005254